BJPS

Brazilian Journal of
Pharmaceutical Sciences

http://dx.doi.org/10.1590/s2175-97902022e201144

Article

Optimization and Quest of HPMC loaded Stavudine Controlled Release Dosage Development by Central Composite Design utilizing Reduced Factorial Screening Technique

Jyothsna Gangolu[1], Sandyapakula Balaiah[1], Sisir Nandi[2], Harekrishna Roy[1*]

[1] Department of Pharmaceutics, Nirmala College of pharmacy, Affiliated to Acharya Nagarjuna University, Andhra Pradesh, India, [2] Department of pharmaceutical chemistry, Global Institute of Pharmaceutical Education and Research, Affiliated to Uttarakhand Technical University, Uttarakhand, India

The current research focused on screening and finding the significant independent variables in stavudine loaded tablet, followed by optimizing the best formulation using central composite design. The objective of the study to develop stavudine loaded controlled release tablet utilizing reduced factorial design, followed by optimization technique as well as characterization of prepared tablets. Preliminary trial batches were prepared using different grades of hydroxypropyl methylcellulose. The resolution-IV reduced factorial design was selected to screen the significant independent variables in the dosage form design. A total number of eight runs were prepared and responses were recorded. The signified factors identified by half-normal and Pareto chart. The prepared tablets are evaluated for various physiochemical characterizations. Three dependent responses such as hardness, dissolution at 6 hour and 12 hours are considered in optimization process. Later on, drug-polymer interaction study was carried out. The principal of the study design based on finding the best formulation with prefixed set parameter values utilizing the concept of screening technique. It observed that HPMC K15M (57.18 %), HPMC K100 (66.32 %) and PVP K30 (7.97 %) as best composition in a formulation batch would fulfill the predetermined parameter with specific values.

Keywords: Stavudine controlled release tablet. Optimization technique. Screening technique. Reduced factorial design. Mathematical modeling.

INTRODUCTION

There have been a lot of challenges while designing a dosage formulation, considering customer satisfaction and predetermined quality assured. The pharmaceutical industry invests a huge capital and time for the successful release of a dosage form to the market (Lee, Choi, 2015; Baranov, Muzyko, 2015; Giaccotto, Golec, Vernon, 2011). Generally, it expenses $950 million and taking around ten years for the successful releasing one to two drug molecules into the market (Hejaz, Karaman, 2015; Roy, Nandi, 2019). It also noted that on successful completion of all phases in a clinical trial; few dosage forms recalled from the market in post-marketing surveillance study (Onakpoya, Heneghan, Aronson, 2015; Onakpoya, Heneghan, Aronson, 2016). Hence, there has been incredible demand for *in-silico* computational and mathematical models for developing a dosage form as well as drug molecule (Kazmi *et al.*, 2019; Shamsi *et al.*, 2019; Ooms, 2000). In general, it can be simply stated that a procedure involves the preparation of a series of formulations with varying concentrations of ingredients (factors) in a scientific and systemic manner (Dokoumetzidis, Kalantzi, Fotaki, 2007; Yu, Wilson, 2010; Saini, Bakshi, Sharma, 2018). The factors used to evaluate using a defined (prefixed) response, and relationships can be understand using suitable models (first order, second

***Correspondence:** Mr. Harekrishna Roy. Department of Pharmaceutics. Nirmala College of pharmacy. Mangalagiri (M), Guntur (Dist), Andhra Pradesh**,** 522503, India. E-mail: hareroy@gmail.com. ORCID ID: https://orcid.org/0000-0001-7211-2528

order) (Prasad *et al*., 2016). In recent decades, there has an increase in demand of *in-silico* screening techniques such as Reduced factorial design (RFD), Placket-Burman design, and Taguchi design can increase the efficiency of the dosage form development process (Koradia, Parikh, Koradia, 2017; Mishra, Mishra, Padh, 2018). Similarly, further in process optimization of a dosage form with concentration can be studied by mixture design, factorial design, box-Behnken design, and central composite design, etc. (Hardikar, Bhosale, 2018; Cheng *et al*., 2018; Roy, 2018).

RFD is one of the screening techniques and belongs to the class of nonparametric methods, in which the number of variables is kept to a reasonable number compared to full factorial design (Jaynes *et al.et al.,*, 2013). An RFD is preferable when resources are limited or the number of factors in the design large; generated from a full factorial experiment by choosing an *alias structure* (Baker *et al.et al.,*, 2017). While carrying out the design study, the desired resolution (Resolution I-VI) must be fixed carefully to separate main effects and low-order interactions from one another (El-Helaly, Habib, El-Rahman, 2018). Response surface methodology belongs to the simulation method; is a three-dimensional geometric representation that establishes an empirical relationship between responses and factors (independent variables). This methodology serves as a powerful for determining the optimal set of experimental conditions that maximize a response (Parhi, Suresh, Patnaik, 2016; Sah, Suresh, 2017).

In the current study, RSM design such as central composite design (CCD) was implemented to fix the experiments as well as to evaluate the optimization of the variables (factors) and responses (Sadhukhan, Mondal, Chattoraj, 2016). The CCD embedded factorial or fractional factorial design contains twice as many star points as factors along with center point in design. The advantage of CCD allows scientist to run the experiment with few number theoretical examination without involvement of complex factorial experiment. It's a popular experimental design for modeling a second-order (quadratic) model for the response (dependent variable) without needing a complete three-level factorial experiment (Aziz, Abdelbary, Elassasy, 2018). A second-order polynomial equation plotted using a small number of experiments and compared one variable at a time in our study.

The world health organization reported around 37.9 million people living with human immunodeficiency virus (HIV) and globally 7,70,000 people died from HIV related causes at the end of 2018. Among all countries, the African region suffered a lot, with 25.7 million people from HIV related complications (World Health Organization. HIV AIDS: Key facts, 2019). Stavudine is a nucleoside reverse transcriptase inhibitor used to treat type -1 HIV and as a combination with other anti-HIV infection drugs. Although it may not be the first line of the drug, it may prevent infection after a needle stick injury or other potential exposure (US National library of medicine. Pubchem: Stavudine, 2019). It rapidly absorb on oral adminstration with bioavailability of 68-104 % but posses negligible protein binding. Stavudine metabolizes intracellularly to stavudine triphosphate and provide short biological half-life (0.8-1.5 h). It have solubility of 83 mg/ml in water and poor solubility in propylene glycol at 23 ^{0}C. Stavudine triphosphate inhibit DNA polymerase and reduces viral mitochondrial DNA (Zerit: Stavudine-FDA, 2021). Controlled release (CR) dosage forms are those, who deliver the medicament for an extended period of time. Hydroxypropyl methylcelluloses (HPMC) are the class of biodegradable hydrophilic polymers currently being extensively used in CR dosage form with blend of two or more grades; differs in molecular weight. The current study discusses CR tablets, as it preferred most accessible dosage form in terms of patient compliance and pharmaceutical industry point of view. There have been significant researches being carried out on stavudine dosage form. But very rare cases reported related to stavudine dosage form utilizing the *in-silico* screening and optimization technique with different grades of HPMC.

Hence, in our study, it investigated and developed a controlled release tablet of stavudine in a scientific approach by computer-operated screening technique with response surface design such as CCD and investigated the effect of variables (factors) on responses with the finding. The novelty of current study is the investigating the significant variables along with optimization and variables study utilizing various grades of high purity (98%) HPMC (E5 LV, E15 LV, K4M, K15M, and K100).

MATERIAL AND METHODS

Material

Chemicals

Stavudine was received as a gift sample from, Mumbai, India (Cipla Ltd.). Different grades of Hydroxypropyl methylcellulose HPMC (E5 LV, E15 LV, K4M, K15M, and K100), Polyvinyl pyrrolidone (PVP K30) were purchased from Loba chemicals, Mumbai, India. Dicalcium phosphate (DCP), Magnesium stearate and talc were procured from Hi-Media India. All the excipients used are of high analytical grade. The screening design and central composite design with mathematical treatment in a polynomial equation were obtained by using statistical package system.

Methods

Preformulation studies

For the effective formulation, preformulation studies were determined for both pure drug and polymeric excipients. The solubility of the drug was assessed in phosphate buffer 6.8. Whereas, micromeritic and physiochemical properties such as flow property, tapped density, bulk density, compressibility, etc. were determined. Drug polymer compatibility was also done by attenuated total reflection (ATR) (Not displayed in the text).

Preparation of preliminary trial batch for controlled release tablets

A total of fourteen tablet formulations were prepared by wet granulation technique (Osamura *et al*., 2019). A formulation requires blend of two or more grades of polymer to qualify the quality control study. Stavudine and different grades of HPMC passed through #40 mesh and mixed well for ten minutes with the required quantity of DCP in a double cone blender (Inoxpa, India). The mixed powder transferred to a pilot-scale granulator, and 5% PVP K30 was poured as a granulating agent. The wet mass granulated for 20 minutes and followed by sieving at # 20 mesh and dried in a hot air oven at 55 ^{0}C for 15 minutes. Finally, the dried granule along with magnesium stearate and talc blended; compressed with a multistation tablet compression machine (Cadmach Tablet Press) with an 8.0 mm circular flat punch. The prepared tablets preliminary evaluated for hardness and disintegration time (DT) to select the possible excipients for further screening study (Table I) (Kyavars, Subramanian, 2018).

TABLE I - Preliminary trial batches for controlled release tablets

Sl.no	Ingredients	Formulations													
		F1	F2	F3	F4	F5	F6	F7	F8	F9	F10	F11	F12	F13	F14
1	Stavudine	20	20	20	20	20	20	20	20	20	20	20	20	20	20
2	HPMC K4M	80	50	50	80	90	60	_	_	_	_	_	_	_	_
3	HPMC K15M	100	50	_	_	_	_	50	100	50	100	100	_	_	_
4	HPMC K100M	_	80	80	50	_	_	60	80	_	_	40	_	60	90
5	HPMC E5 LV	_	_	50	_	_	80	70	_	80	_	40	100	60	90
6	HPMC E15 LV	_	_	_	50	90	40	_	_	50	80	_	80	60	_
7	PVP K30 (5%)	q.s	q.s	q.s	q.s	q.s	q.s	q.s	q.s	q.s	q.s	q.s	q.s	q.s	q.s
8	Dicalcium phosphate	90	90	90	90	90	90	90	90	90	90	90	90	90	90
9	Mg stearate	5	5	5	5	5	5	5	5	5	5	5	5	5	5
10	Talc	5	5	5	5	5	5	5	5	5	5	5	5	5	5
	Total weight(mg)	300	300	300	300	300	300	300	300	300	300	300	300	300	300

Factor screening study

The screening of factors while preparing the promised tablet dosage form was performed by reduced factorial design (RFD) (Durakovic, 2017; Rezende *et al*., 2018). The objective of the factorial screening study was needed to identify the possible significant independent variables while eliminating the non-responsive variable in the optimization study design. The resolution-IV for 2^{4-1} RFD was selected, in which HPMC K4M, HPMC K15M, HPMC K100, and PVP K30 selected as independent variables and a total eight number of runs finalized. The responses were monitored, such as hardness, dissolution release at 6 h and 12 h (Table II). The obtained data subjected to analysis with the help of statistical modeling; the process order was design model, and model type considered as factorial. During the study finding the factors signifying the responses was identified by the half-normal plot and Pareto chart.

TABLE II - Screening run batches suggested by reduced factorial design

Run	Factor 1	Factor 2	Factor 3	Factor 4	Response 1	Response 2	Response 3
	A:HPMC K4M (mg)	B:HPMC K15M (mg)	C:HPMC K100 (mg)	D:PVP K30 (%)	Hardness (Kg/cm^2)	Dissolution (6 h) (%)	Dissolution (12 h) (%)
1	**40**	**50**	**90**	**10**	**6**	**71.9**	82.6
2	60	100	40	5	5	72.1	81.9
3	40	100	90	5	4.5	81.2	98.9
4	60	50	90	5	4	78.3	94.7
5	40	50	40	5	3	72.8	87.2
6	40	100	40	10	3.5	77.3	92.1
7	60	50	40	10	3	74.6	83.7
8	60	100	90	10	4	68.5	80.6

Optimization study

The optimization of the controlled release stavudine tablet was assessed by response surface study type. The factors considered in this technique were identified by factor screening study. A total of twenty runs developed by central composite design (CCD) with three factors and two-level studies (Table III). The responses were studied and characterized are hardness, dissolution at 6h, and 12 h. Mathematical fitting and analysis were performed by the polynomial equation (Kassem, Shaboury, Mohamed, 2019; Qu, Venter, Haftka, 2004). The validation and model fitting such as quadratic and linear was evaluated by *p*-value, adjusted R^2, and predicted R^2 values. The simulations of all responses with the desired factors are characterized by 3D-response surface and 2D-contour plot design. The optimized formula was solved by graphical optimization technique along with a numerical method using the confidence interval value of alpha 0.05. The desired value was fed with lower and upper value to ascertain the optimized. Moreover, the overlay plot was assessed to locate the design space.

TABLE III - Batches suggested by central composite design for optimization study

Run	Factor 1	Factor 2	Factor 3	Response 1	Response 2	Response 3
	A: HPMC K15M (mg)	B: HPMC K100 (mg)	C: PVP K30 (%)	Hardness (kg/cm^2)	Dissolution (6 h) (%)	Dissolution (12 h) (%)
1	50	90	10	5.5	72.35	90.12
2	32.9552	65	7.5	3	72	89.6
3	50	90	5	3.5	71.05	87.12
4	75	65	11.704482	5	65.36	84.65
5	75	65	7.5	4.5	62.76	83.35
6	75	65	7.5	4	65.6	84.15
7	75	65	7.5	4.5	69.95	85.36
8	75	107.04482	7.5	5.5	69.15	84.19
9	75	65	7.5	4	69.25	84.97
10	50	40	10	2.5	72.8	91.7
11	75	65	7.5	5.5	67	86.05
12	117.045	65	7.5	5.5	60	81.75
13	75	65	7.5	5	69.25	85.23
14	50	40	5	3	76.1	91.05
15	100	90	10	6.5	65.6	81.78
16	100	40	10	4.5	75.9	85.7
17	75	22.955179	7.5	3.5	79.1	95.3
18	100	40	5	3.5	79.1	94.27
19	100	90	5	4.5	53.05	73.79
20	75	65	3.2955179	4.5	60.15	82.2

Characterization of matrix tablets suggested by CCD

The physical properties like hardness, friability, thickness, diameter, weight variation, drug content, and swelling index for every run were determined and provided in Table IV (Aslani, Sharifian, 2014). Generally, the strength of the tablet depends on the friability and hardness study. Tablet hardness was determined by considering ten tablets using Monsanto tablet hardness tester (Dolphin, India). To find out the tablets for resisting the wears and tears, the friability test was performed using Roche friabilator. The predetermined tablets were kept and rotated at 100 revolutions. The diameter and thickness of tablets were measured by the digital vernier caliper scale (Mitutoyo, 500-719, India). For weight variation, twenty tablets were weighed on a digital balance (Shimadzu TX 423L) and final weight provided in Table IV, the percentage weight differences were calculated. The densities of the prepared mixture were also determined by a standard glass cylinder — the drug content regarding an assay performed as per Indian Pharmacopoeia (IP) of every batch determined in triplicate. For every batch, twenty tablets were weighed and crushed to a fine powder by mortar and pestle.

Accurately weighed of 20 mg of the equivalent powder was taken and dissolved in methyl alcohol and analyzed by UV spectrophotometer (Double beam UV Visible Spectrophotometer SL 210, Elico). The swelling index was performed in a Petri plate. Pre weighed tablets are placed in Petri plates and filled with phosphate buffer 6.8. At a specific time interval, the final weight of the tablet was determined, and the differences are reported as the percentage of swelling.

Swelling index=(Wt-W0)/W0 x 100 (Equation 1)

Where Wt=final weight of tablet at time "t" and W0=initial weight of the tablet.

TABLE IV - Characterization of prepared tablets suggested by CCD

Run	Thickness (mm)	Diameter (mm)	Friability (%)	Weight variation (mg)	Hardness (Kg/cm²)	Drug content (%)	Swelling index at 6h (%)	Swelling index at 12h (%)
1	4.19±0.043	8.09±0.063	0.234±0.01	305.45±1.58	5.5±0.2	93.55±1.2	73.12±2.34	77.73±3.08
2	4.01±0.041	8.13±0.083	0.296±0.02	303.05±0286	3±0.9	91.231.5	68.87±3.17	76.53±5.16
3	4.34±0.043	8.02±0.063	0.123±0.01	304.20±1.37	3.5±0.8	96.10±1.3	73.24±4.21	76.89±1.97
4	4.17±0.041	8.1±0.052	0.356±0.01	303.10±3.52	5±0.5	99.25±2.1	73.36±1.55	79.18±6.31
5	4.23±0.046	8.02±0.023	0.358±0.03	301.30±1.94	4.5±0.4	94.29±2.5	73.12±4.01	77.89±3.63
6	4.15±0.049	8.12±0.065	0.215±0.05	305.95±2.58	4±0.1	94.56±1.5	73.81±3.54	80.93±2.62
7	4.22±0.059	8.05±0.065	0.325±0.01	302.95±1.25	4.5±0.5	91.72±2.4	71.75±3.25	78.74±3.04
8	4.38±0.023	8.07±0.056	0.395±0.05	303.40±1.63	5.5±0.8	96.43±1.5	74.58±2.79	80.75±4.72
9	4.15±0.045	8.1±0.064	0.213±0.04	301.95±2.58	4±0.5	97.43±2.0	74.15±1.48	77.06±1.28
10	3.97±0.063	8.60±0.065	0.389±0.05	302.30±0.18	2.5±0.8	92.72±1.6	71.09±4.07	75.69±4.73
11	4.19±0.046	8.59±0.068	0.248±0.01	304.20±0.49	5.5±0.5	95.19±2.5	74.36±1.57	78.13±3.76
12	4.30±0.063	8.10±.065	0.221±0.03	303.20±3.84	5.5±0.8	99.61±2.0	75.86±3.89	79.59±2.44
13	4.21±0.064	8.07±0.068	0.156±0.05	306.60±2.59	5±0.7	91.36±1.5	73.36±1.79	78.13±3.75
14	4.07±0.052	8.02±0.060	0.284±0.06	305.65±0.81	3±0.7	90.43±3.0	68.71±3.72	74.68±2.45
15	4.42±0.051	8.07±0.062	0.165±0.04	302.80±1.73	6.5±0.1	92.61±2.5	74.58±1.38	80.19±1.54
16	4.18±0.032	8.03±0.063	0.389±0.02	303.60±2.78	4.5±0.5	98.94±1.5	73.01±4.15	78.67±4.85
17	4.09±0.065	8.05±0.064	0.289±0.01	305.35±1.28	3.5±0.5	91.78±3.0	70.81±3.67	74.41±3.64
18	4.27±0.045	8.20±.064	0.156±0.05	304.75±1.54	3.5±0.8	97.81±2.5	73.12±2.78	75.98±1.75
19	4.33±0.042	8.08±0.056	0.198±0.01	305.74±0.98	4.5±0.1	98.84±1.0	75.62±1.73	79.54±4.2
20	4.11±0.041	8.08±0.061	0.352±0.03	301.6±2.72	4.5±0.9	96.84±1.5	72.14±3.17	76.55±3.51

Data shown are the mean ± standard deviation (n=3)

In-vitro dissolution study

The study was carried out in the United States Pharmacopoeia (USP) dissolution testing apparatus type-II (paddle method). The dissolution beaker was filled with 900 ml of 0.1N HCl (pH-1.2) for an initial 2 h and followed by phosphate buffer pH 6.8 for another 10 h. The bath temperature was maintained at 37 ± 0.5°C, and paddles were fixed at 50 rpm. An aliquot sample of 5 ml of the solution was withdrawn from time to time with a predetermined interval and replaced with a fresh dissolution medium (Simionato *et al.*, 2018). The samples were passed through a 0.45 µm membrane filter and diluted to suitable concentration. The absorbance

of those solutions was measured at lambda max 267 nm using a Double beam UV Visible Spectrophotometer (SL 210, Elico).

Fourier transform infrared (FTIR) spectroscopy study

Generally, potential interaction between drug and excipients are being carriedout by FTIR analysis. An approximately 1% of sample mixed with 200 mg of KBr and put in a pellet forming die. Approximately 5 tons of pressure applied under vaccum for several minute. The prepared pellet subjected to infrared spectroscopy analysis. The peaks were recorded (drug, excipients and optimized formula) and analyzed for appearance and position (Huang, Wigent, Schwartz, 2008).

Differential scanning colorimetry (DSC) study

DSC technique find the behavior of material (melting temperature, crystallization, glass transition etc.) in respect to change in temperature. It is a thermo analytical technique records appearance and disappearance of peak interms of endothermal and exothermal peak (Attia, Abdel-Moety, Abdel-Hamid, 2017). Around 100 mg of sample placed in sample holder as a thin layer. An empty sample pan kept as reference; as it cancels the heat flow to and from the pan.Care must be taken that, no such heat exchange take place between sample and surrounding.

X-ray diffraction (XRD) technique

XRD technique defines the crystallographic changes especially in crystalline substances. The working principle based on constructive interference from a source of monochromatic X-ray and crystalline sample following Bragg law. The spectrum obtained by plotting a graph between ionization current and "θ" angle (Lennox, 1957).

RESULTS AND DISCUSSION

Preformulation studies

The preformulation study indicated the solubility of stavudine is 89 mg/mL in phosphate buffer pH 6.8. The drug was excellent soluble in ethyl alcohol and methyl alcohol. The micromeritic and derived property values for granules exhibited good to compact and superior flow property (Not displayed in the text).

Preliminary screening of trial batches

In our preliminary study, we prepared fourteen trial formulas as per the literature survey, considering the appropriate proportion of polymers such as HPMC K4M, HPMC K15M, HPMC K100, HPMC E5 LV, and HPMC E15 LV. Table I describes the best possible combination of a dosage form in our study. The prepared trial batched especially evaluated for hardness and disintegration study. It observed, the batch containing HPMC E5 LV and HPMC E15 LV were poor in strength and disintegrated within 60 minutes. This confirmed and selected remaining polymers such as HPMC K4M, HPMC K15M, HPMC K100 and PVP K30 for further factorial screening and optimization study.

Factor screening study

The screening of influential factors as main effects were assessed by RFD with randomized subtype considering a total of eight numbers of runs as displayed in Table II. The model fitting for the data obtained by the formulations is validated by factorial type, indicated good fitness for main effect determination. Linear polynomial equations are constructed, and the synergistic and antagonistic factors are evaluated (Arinkoola, Ogbe, 2015; Hooda *et al*., 2012).

Hardness= 4.125 – 0.125A + 0.125B + 0.5C – 1.327D + 0.375 AB -0.5AC -0.5AD (Equation 2)

Dissolution (6h)= 74.58 – 1.21A +0.18B+ 0.38C -1.51D -3.26 AB (Equation 3)

Dissolution (12h)= 87.71- 2.48A+ 0.66B+1.48 C -2.96D -4.63 AB +0.93 AC (Equation 4)

In the above-mentioned equations, the positive (+) sign indicates synergistic and negative (-) sign indicated

antagonistic effects. The model suggested the significant factors (highlighted bold) in a term related to the level of the *p*-value. However, it observed interaction terms such as "AB," "AC" also included, but neglected due to chance of aliasing.

Furthermore, the significant main effects were also identified by the half-normal plot and Pareto chart (Figure 1). For the response, hardness is significantly affected by "B" and "C" (HPMC K15M and HPMC K100). In the case of "Dissolution (6 hrs)" greatly signified again by "B" and "C" (HPMC K15M and HPMC K100). For the response variable "Dissolution (12 hrs)", the factor "B," "C" and "AC" exhibited a significant effect. While selecting the main factors, it was more challenging to properly find out the significant main effect of further optimization study. As can be seen for response-1 and response-2 the factors are below the "t value" and "Bonferroni limit," but the statistical software clearly differentiated the positive effect in terms of "orange" color. While for response-3, the main effect effects were above the "t value" and "Bonferroni limit." Hence, it revealed factors "B," "C," and "D" (Binder, PVP K30) were significant and considered for response variables. In furthermore steps, the optimization procedure was carried out by response surface method.

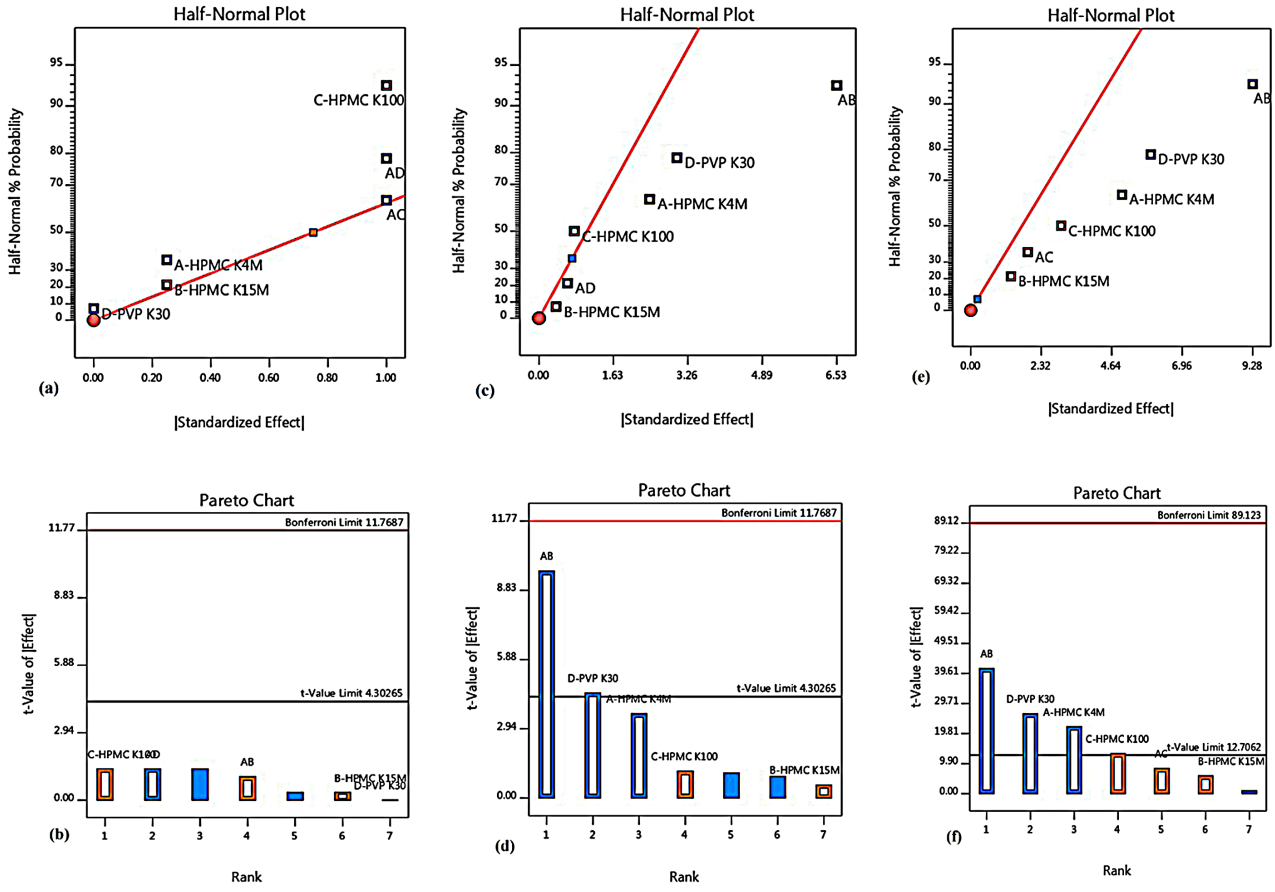

FIGURE 1 - (a) Half-normal plot for "response-1" with influence by factors considered in screening design, (b) Pareto chart for "response-1" with influence by factors considered in screening design, (c) Half-normal plot for "response-2" with influence by factors considered in screening design, (d) Pareto chart for "response-2" with influence by factors considered in screening design, (e) Half-normal plot for "response-3" with influence by factors considered in screening design, (f) Pareto chart for "response-3" with influence by factors considered in screening design.

Factor optimization study

Table III enlisted a total number of twenty runs suggested as per the central composite design. The obtained values subjected to a randomized quadratic model with a response surface study type. On suitability, polynomial equations were plotted for individual responses. Furthermore, the model suitability was also validated by analysis of variance (ANOVA) with significant *p*-value ($p< 0.05$). It showed those quadratic models selected for the study are significant with *p*-values 0.004, 0.002 and 0.0001 for response-1, response-2 and response-3 respectively as displayed in Table V.

TABLE V - Model suitability for CCD by ANOVA

ANOVA data for Hardness (R1)						
Source	Sum of squares	df	Mean	F-value	p-value	
Model	17.1753978	9	1.908378	6.1075855	0.0045794	significant
A-HPMC K15M	5.54798395	1	5.547984	17.755809	0.0017892	
B-HPMC K100	7.1239189	1	7.123919	22.799442	0.0007515	
C-PVP K30	2.08870755	1	2.088708	6.684715	0.0271597	
Adjusted R^2	0.7075	CV%	12.70	Adequate precision	10.04	
Predicted R^2	0.5279	R^2	0.8461			
ANOVA data for dissolution at 6 h (R2)						
Model	726.081363	9	80.67571	7.4767354	0.0020823	significant
A-HPMC K15M	110.412431	1	110.4124	10.232628	0.0095103	
B-HPMC K100	251.307226	1	251.3072	23.290253	0.0006959	
C-PVP K30	19.0088487	1	19.00885	1.761672	0.2139207	
Adjusted R^2	0.7542	CV%	4.78	Adequate precision	12.79	
Predicted R^2	0.5718	R^2	0.8706			
ANOVA data for dissolution at 12 h (R3)						
Model	427.247681	9	47.47196	14.11194	0.0001422	significant
A-HPMC K15M	103.807116	1	103.8071	30.85863	0.0002424	
B-HPMC K100	172.912928	1	172.9129	51.40164	3.03E-05	
C-PVP K30	3.78577251	1	3.785773	1.1253925	0.3137095	
Adjusted R^2	0.8613	CV%	2.13	Adequate precision	15.71	
Predicted R^2	0.6209	R^2	0.9270			

Applying uncoded values of factor levels, the least square regression method was performed using the statistical software for the estimation of coefficients in the polynomial function. The models were statistically validated by p-value, adjusted R^2, and predicted R^2 values (Table V).

$$\text{Hardness} = 4.4 + 0.63A + 0.72B + 0.39C \quad \text{(Equation 5)}$$

$$\text{Dissolution (6h)} = 67.20 - 2.84A - 4.28B + 1.17C - 3.85AB + 1.41AC + 2.54BC + 0.19A^2 + 3.06B^2 - 0.95C^2 \quad \text{(Equation 6)}$$

$$\text{Dissolution (12h)} = 84.83 - 2.75A - 3.55B + 0.52C - 2.36AB - 0.52AC + 2.36BC + 0.41A^2 + 1.85B^2 - 0.38C^2 \quad \text{(Equation 7)}$$

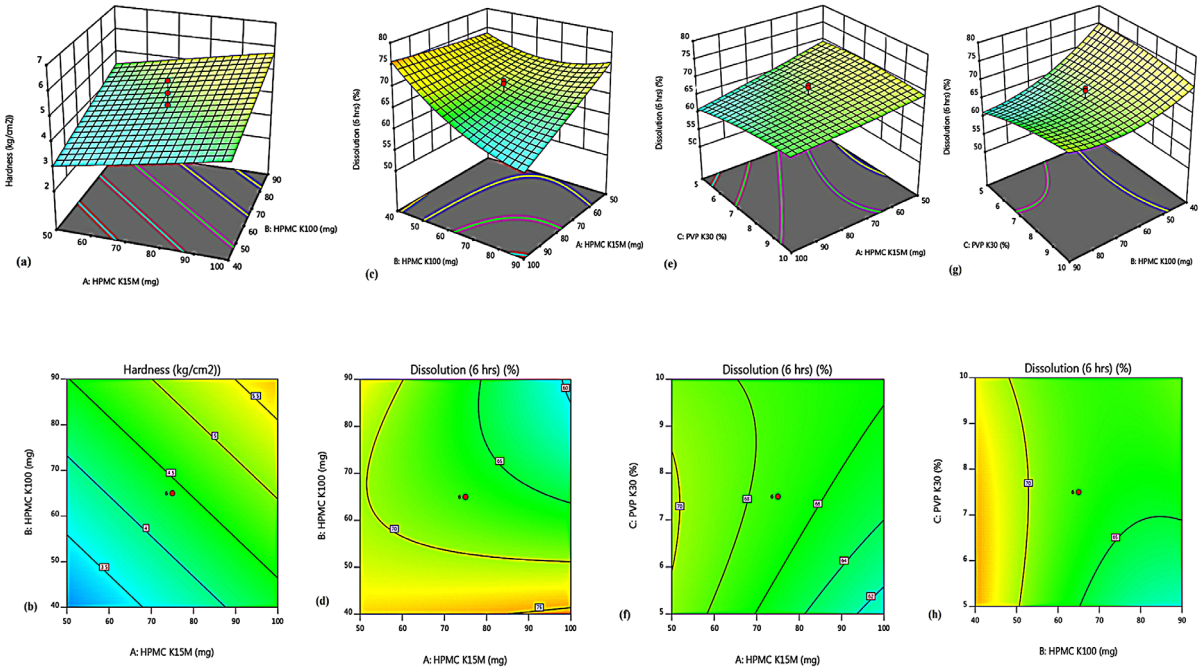

FIGURE 2 - (a) 3D response surface plot for "response-1" (b) 2D contour plot for "response-1" (c) 3D response surface plot for "response-2" obtained by "A" Vs "B" (d) 2D contour plot for "response-2" obtained by "A" Vs "B" (e) 3D response surface plot for "response-2" obtained by "A" Vs "C" (f) 2D contour plot for "response-2" obtained by "A" Vs "C" (g) 3D response surface plot for "response-2" obtained by "B" Vs "C" (h) 2D contour plot for "response-2" obtained by "B" Vs "C".

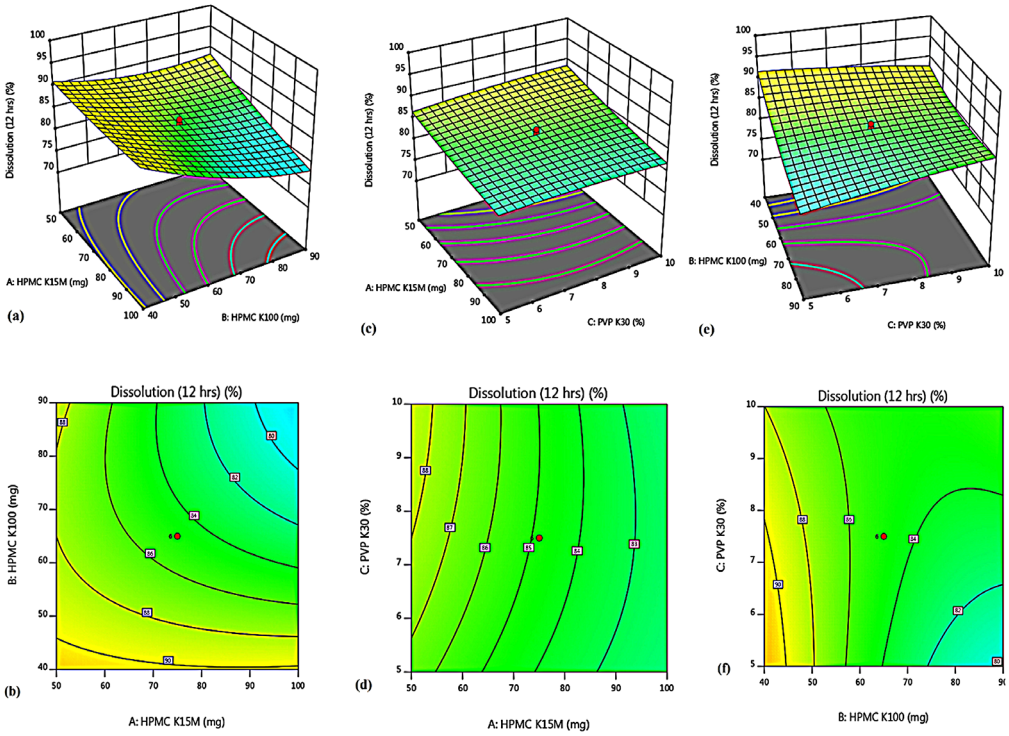

FIGURE 3 - (a) 3D response surface plot for "response-3" obtained by "A" Vs "B" (b) 2D contour plot for "response-3" obtained by "A" Vs "B" (c) 3D response surface plot for "response-3" obtained by "A" Vs "C" (d) 2D contour plot for "response-3" obtained by "A" Vs "C" (e) 3D response surface plot for "response-3" obtained by "B" Vs "C" (f) 2D contour plot for "response-3" obtained by "B" Vs "C".

The quadratic model was best fitted which has been observed in equations of 6 and 7. Hence in the polynomial equation, the quadratic as well as interaction terms were included. Whereas, in equation 5, only the linear terms such as coefficients of A, B, and C as per the model validation procedure. The cubic and quadratic models eliminated as a result of the chance of aliasing.

As per CCD, 3D-response surface and contour plots were plotted in order to investigate the independent factors and responses (Figures 2, 3)

For all runs, the hardness of tablets ranged from 3.0 kg to 6.5 kg. The Figure 2 (a and b) depicted the relationship between response-1 (hardness) and concentration of A and B. It observed that there is no such remarkable significant relationship between the factors and responses as confirmed in equation 5, indicated only linear relationship between HPMC K15M, HPMC K100, and PVP K30. The concept related to response 2: dissolution (6h) illustrated in Figure 2 (c-h) with 3D-response and 2D-contour plots. It observed there was a significant effect of interaction between factors and quadratic terms. The percentage of drugs that underwent dissolution ranged from 53.05% to 79.1%. As the value for factors A and B were 94.63 and 86.74, respectively, the response found 61.04%. For the values of 53.85 mg of A and 86.09 mg of B, the response value increased to 71.30%. Whereas, it observed 74.82% of drug dissolution for the concentration of 94.96 mg of A and only 41.24 mg of factor B. This clearly indicated the significant effect of interaction between factors as well as quadratic values. The pattern also can be seen in plots considering A with C and B with C. In Figure 3 (a-f) illustrated the relationship between all factors to the response-3(dissolution 12h). The predictive value of 87.88% for dissolution at 12hrs observed when the HPMC K100M and PVP K30 were at 41.17 mg and 9.91% respectively. A similar pattern was also observed to 80.72% of dissolution at 12 hrs for 86.73 mg of HPMC K100 and 5.41 % of PVP K30. A significant increase in the predictive result was observed for response-3 at 90.15% at 43.77 mg HPMC K100 and 5.42 % of PVP K30. This result justified obvious significant interaction between factors; moreover, the curvilinear response surface confirmed the interaction effect between factors.

Apart from the response surface methodology, few more model diagnostic tools were analyzed to fit the model for the study. Figure 4 (a-f) highlighted the model diagnostic methodology named Box-Cox plot and Cook´s Distance and confirmed the highest fitting of data in selected models.

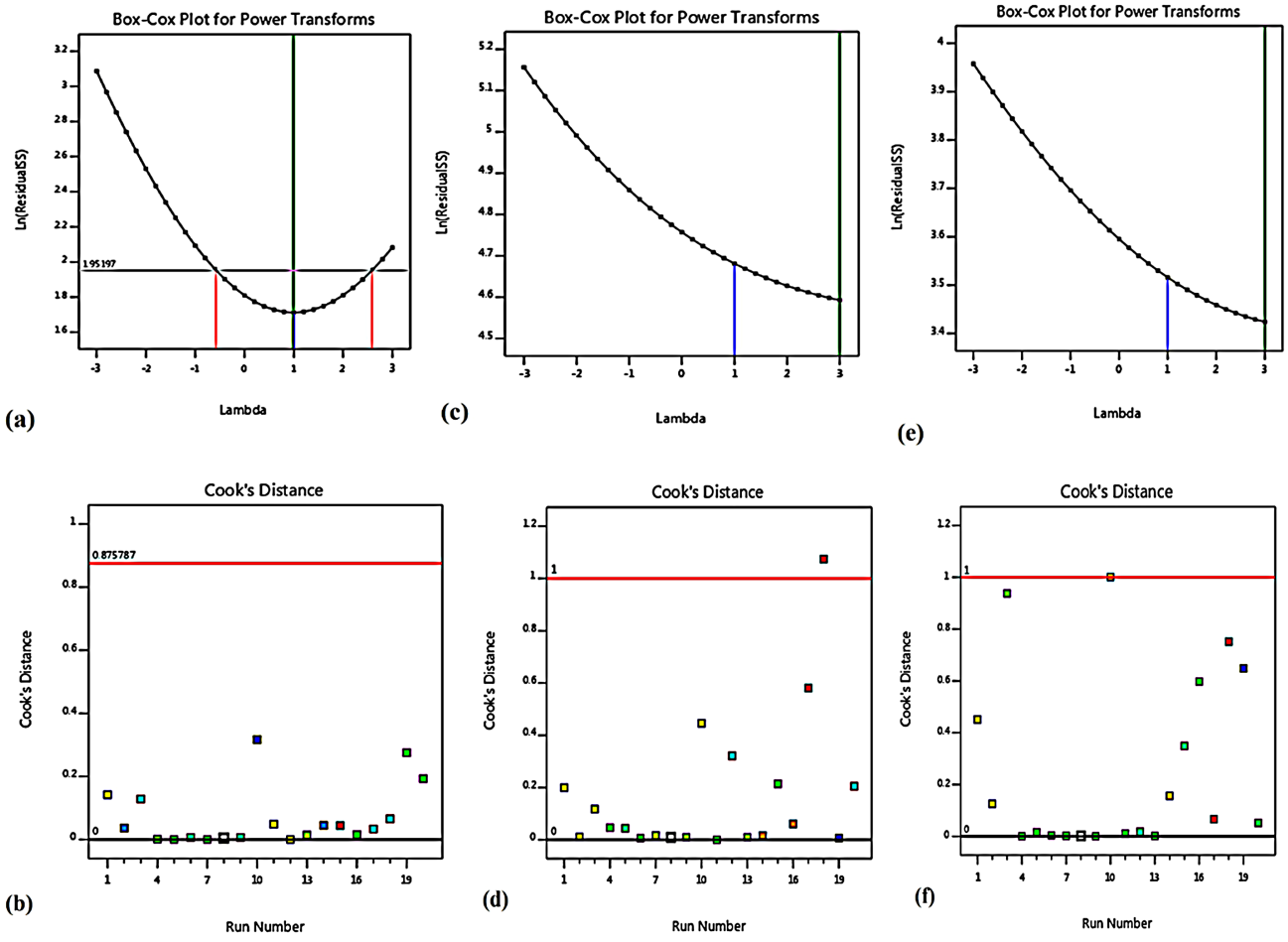

FIGURE 4 - (a) Box-cox plot for "response-1" with influence by factors considered in model study, (b) Cook´s distance chart for "response-1" with influence by factors considered in model study, (c) Box-cox plot for "response-2" with influence by factors considered in model study, (d) Cook´s distance chart for "response-2" with influence by factors considered in model study, (e) Box-cox plot for "response-3" with influence by factors considered in model study, (f) Cook´s distance chart for "response-3" with influence by factors considered in model study.

In-vitro dissolution study

The formulation runs as per CCD suggested, subjected to *in-vitro* dissolution study in pH 1.2 buffer for the initial two hrs and followed by another ten hours in phosphate buffer pH 6.8 displayed in Figures 5 and 6. Remarkably all the formulations extended satisfactory drug release for a time period of 12 h. All the formulations released a minimum of 80 % at the end hours, whereas there were some differences observed because of different compositions in runs. The result showed run numbers 2, 7, 13, 14, and 18 were released 90 % in 12 h of dissolution. In earlier literature review revealed that, HPMC K100 has lesser apparent viscosity of 80-120 cP as compared to HPMC K15M, which has apparent viscosity of 11250-21000 (Using METHOCEL cellulose ethers for controlled release of drugs in hydrophilic matrix systems, 2019). As it can be seen from the run 15, it released 81.78 % of the drug whereas 85.7% of dissolution from run number 16 at the end of 12 h. It clearly observed that the percentage extent release of a drug depends on the viscosity and concentration of polymers. Run number 18 released 94.27% of the drug; meanwhile, run 16 released only 85.7 % of the drug; this could be attributed by a higher percentage of PVP K30 in formulation number 16 (run 16).

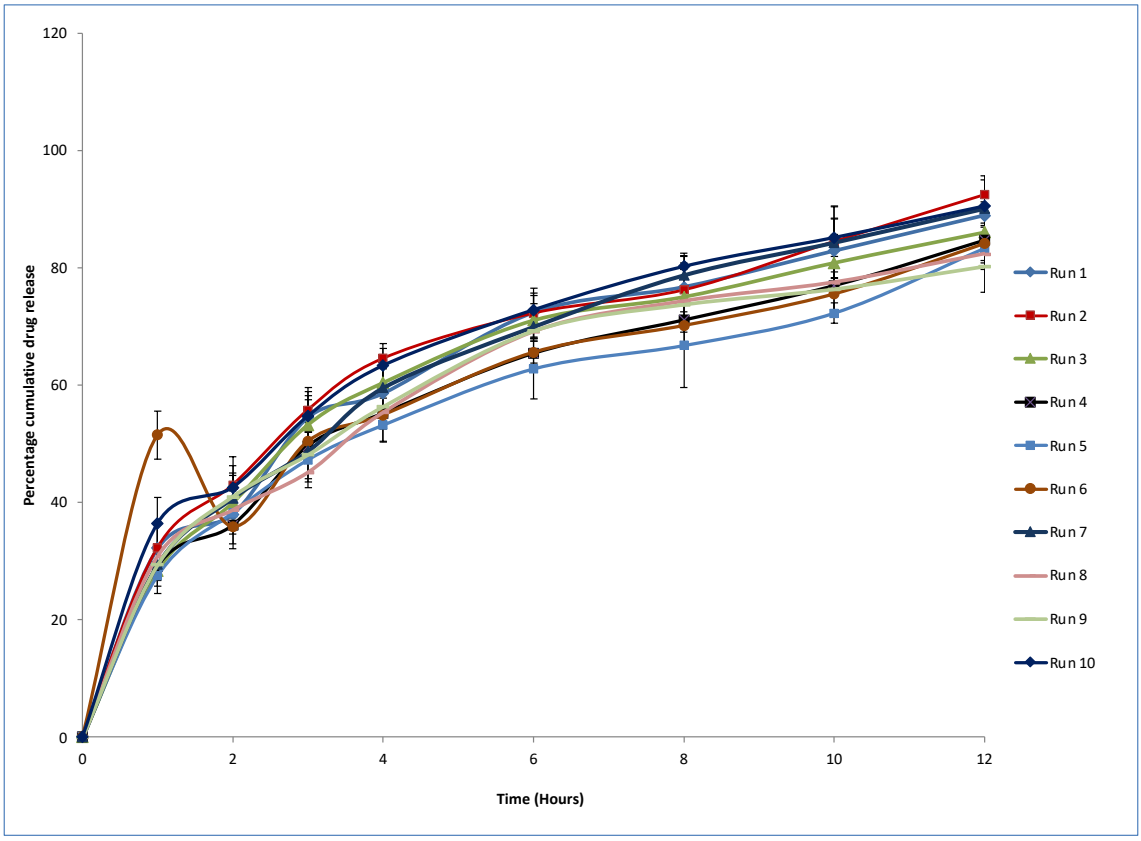

FIGURE 5 - In-vitro drug release for run 1-run10 suggested by CCD.

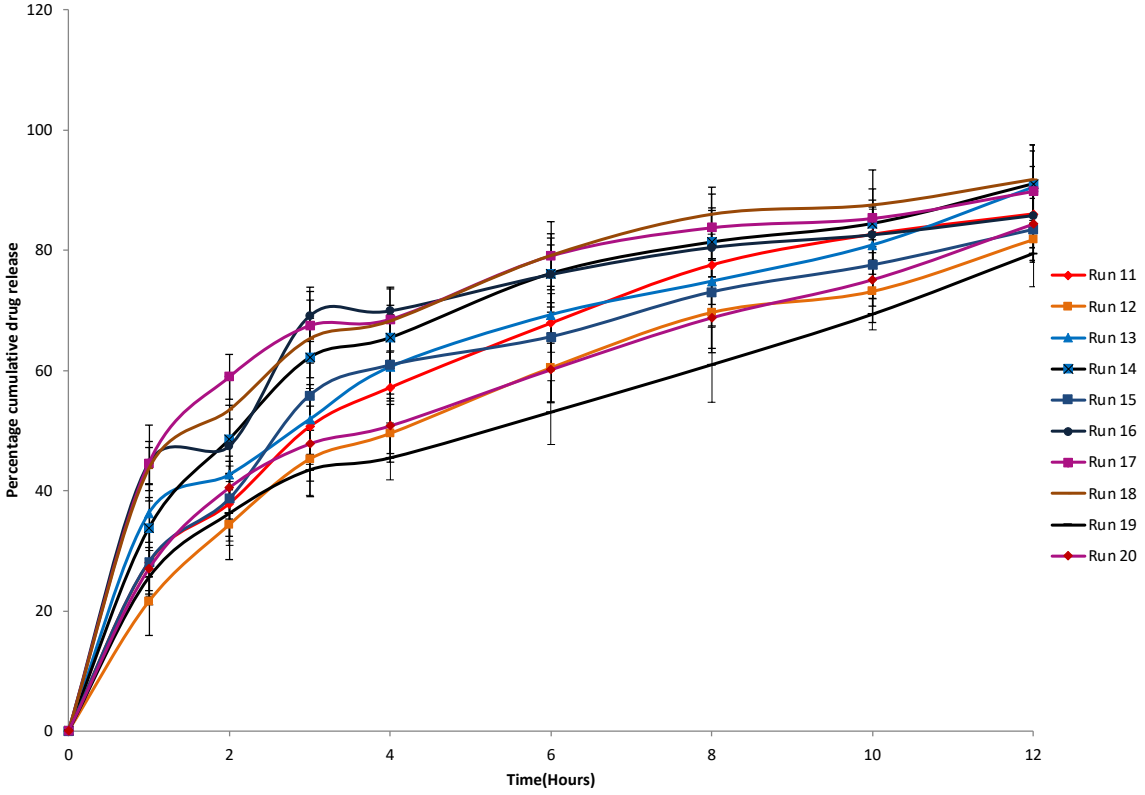

FIGURE 6 - In-vitro drug release for run 11-run 20 suggested by CCD.

Optimizing the formulation

The optimized matrix tablet formulation was identified by close characterization observation from all the runs suggested by CCD. The final optimal experimental parameters calculated using the canonical analysis, which allowed to compromise among various responses and searches for a combination of factor levels that jointly optimize a set of responses by satisfying the requirements for each response in the set. The graphical method of optimization followed by the numerical method was adopted to find out the predetermined set of optimized formulation, followed by concentration findings from the numerical method of optimization. The 3D and 2D graphical method of optimization acted as simulation to find out the best and optimized formulation. Further, the robustness of the optimized is confirmed by the design space. The design space was marked in the yellow color region in an overlay plot, as shown in Figure 7 (a)-7 (c) (Hasniyati, Zuhailawati, Ramakrishnan, 2016; Sathish *et al*., 2018). The optimized formulation found to be an exhibit by HPMC K15M (57.18 %), HPMC K100 (66.32 %) and PVP K30 (7.97 %) with predicted value of hardness (4.05 mg), dissolution at 6hrs (69.27 %) and dissolution at 12 hrs (87.09 %). Furthermore, the optimized formulation and concentrations of independent variables confirmed, in order to fulfill the optimization process by desirability function analysis (DFA). To perform DFA, the target values fed for three responses; Later on desirability values obtained in combined effect of HPMC K15M, HPMC K100 and PVP K30 as displayed in Table VI.

TABLE VI - Results of desirability function analysis

Number	HPMC K15M (mg)	HPMC K100 (mg	PVP K30 (mg)	Hardness (kg/cm^2)	Dissolution (6 h, %)	Dissolution (12 h, %)	Desirability
1	62.40	58.34	8.54	4.05	69.26	87.11	1
2	86.25	51.81	5.86	4.06	69.26	87.08	1
3	57.18	66.32	7.97	4.05	69.27	87.09	1
4	62.47	58.25	8.56	4.05	69.27	87.09	0.9997
5	57.20	66.16	7.94	4.04	69.28	87.08	0.9996
6	62.11	58.69	8.52	4.05	69.25	87.09	0.9996
7	61.94	58.91	8.51	4.04	69.24	87.08	0.9994
8	57.10	66.34	7.93	4.05	69.28	87.09	0.9994
9	61.79	59.11	8.51	4.04	69.23	87.09	0.9993
10	86.50	51.81	5.82	4.04	69.22	87.08	0.9990
11	58.33	64.26	8.11	4.04	69.21	87.09	0.9989
12	58.64	63.76	8.1	4.05	69.21	87.09	0.9987
13	60.86	60.37	8.42	4.05	69.20	87.09	0.9986
14	60.36	61.09	8.37	4.04	69.19	87.09	0.9984
15	59.47	62.42	8.26	4.04	69.19	87.09	0.9983
16	59.77	61.97	8.31	4.04	69.18	87.09	0.9983
17	62.75	58.71	8.53	4.06	69.21	87.01	0.9946
18	65.48	51.92	9.71	4.12	69.26	87.09	0.9896

TABLE VI - Results of desirability function analysis

Number	HPMC K15M (mg)	HPMC K100 (mg	PVP K30 (mg)	Hardness (kg/cm^2)	Dissolution (6 h, %)	Dissolution (12 h, %)	Desirability
19	69.01	57.05	7.71	4.04	69.27	86.64	0.9887
20	71.63	56.28	7.42	4.05	69.26	86.57	0.9868
21	74.97	55.28	7.06	4.05	69.27	86.55	0.9863
22	74.05	55.56	7.15	4.04	69.28	86.56	0.9863
23	52.57	74.53	7.15	4.04	69.89	87.08	0.9781

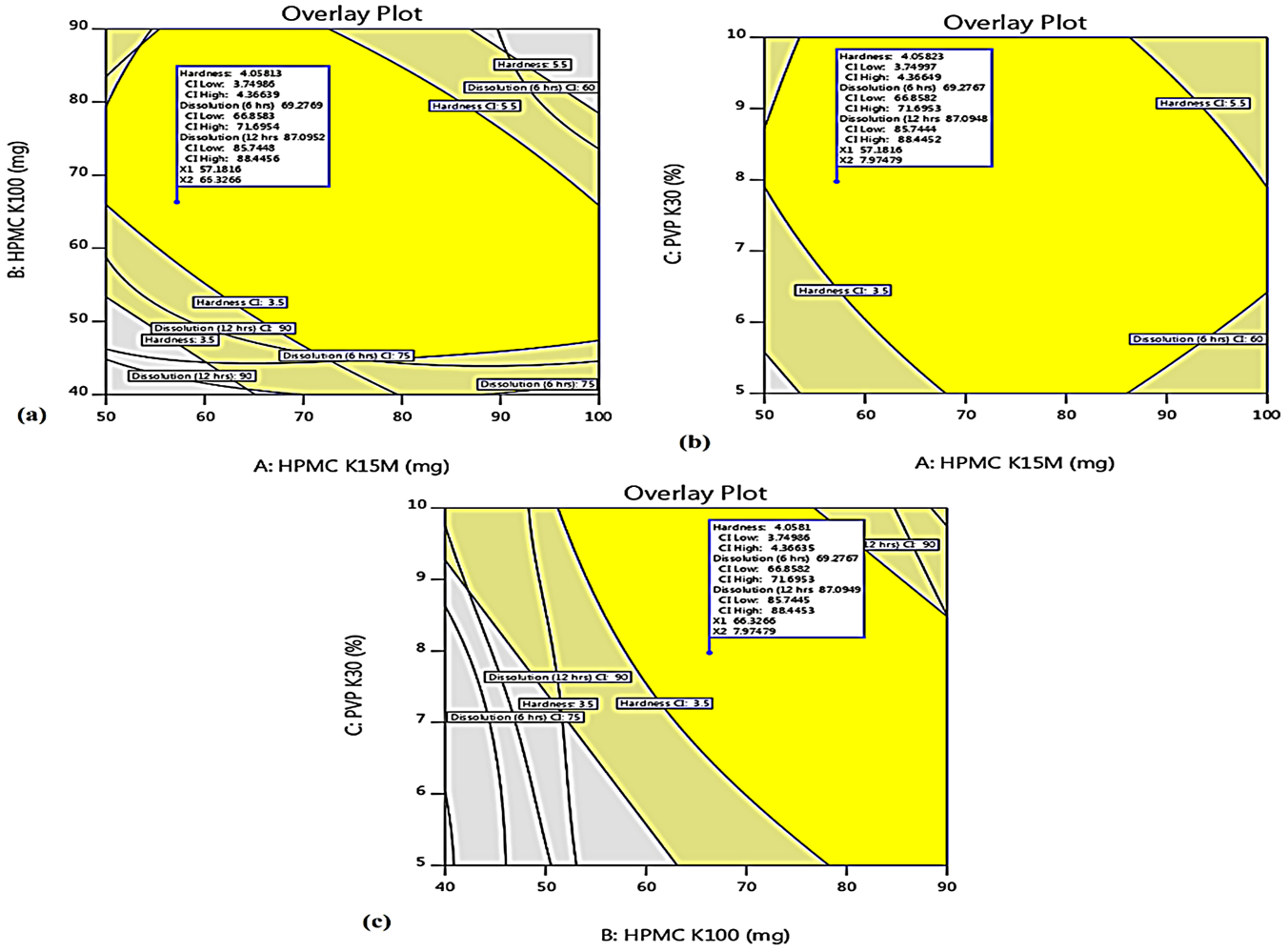

FIGURE 7 - Overlay plot for finding the optimizing region as per predetermined set value for (a) Hardness, (b) Dissolution (6 h) (c) Dissolution (12 h).

Finally, the confirmation batch, as suggested prepared and responses observed. Table VII provided data for a high degree of closeness between predicted and the observed value of the response; confirmed the excellent closeness in terms of responses between the mathematically derived optimized and final confirmed

batch. The optimized batch subjected to *in-vitro* dissolution and kinetics study ascertained. The release data followed zero order kinetics and obeyed higuchi diffusion mechanism (Data not provided in the text). Futhermore, optimized batch subjected to drug-polymer interaction study.

TABLE VII - Measured responses observed of optimized formula as per obtained by oveylay plot

Response	Predicted	Observed	Std Dev	SE Mean	95% CI low	95% CI high	95% TI low	95% TI high
Hardness	4.05832	**4.5**	0.5884	0.17656	3.68403	4.43262	1.60151	6.51514
Dissolution (6 h)	69.2766	**72.52**	3.28485	1.33439	66.3034	72.2498	53.3787	85.1744
Dissolution (12 h)	87.0947	**90.71**	1.83411	0.74506	85.4346	88.7548	78.2181	95.9713

Drug-polymer interaction study

Fourier transform infrared (FTIR) spectroscopy

The Fourier transform infrared spectrophotometer FTIR (FTIR 8400S, Shimazu) with potassium bromide (KBr) pellets was used to trace out as well as to identify the possible interaction between drug and polymers (Huang, Wigent, Schwartz, 2008*).* As illustrated in Figure 8 (e), the characteristic peaks for pure drug displayed. The characteristic peaks for ether and diaryl ketone exhibited at 2819.64 cm^{-1} and 1697.71 cm^{-1} respectively. A sharp peak was observed at 1460.53 cm^{-1} for the presence of hydrocarbon (C=C), whereas a sharp and distinct peak pointed at 3426.58 cm^{-1} for secondary amine (N-H). The peaks at 2819.64 cm^{-1} and 1460.53 cm^{-1} appeared for the presence of hydroxyl (-OH) and cyanide (CN) groups respectively. The optimized formula, as suggested in Figure 8 (d), FTIR spectra compared with pure drug and revealed there was no such remarkable difference between them.

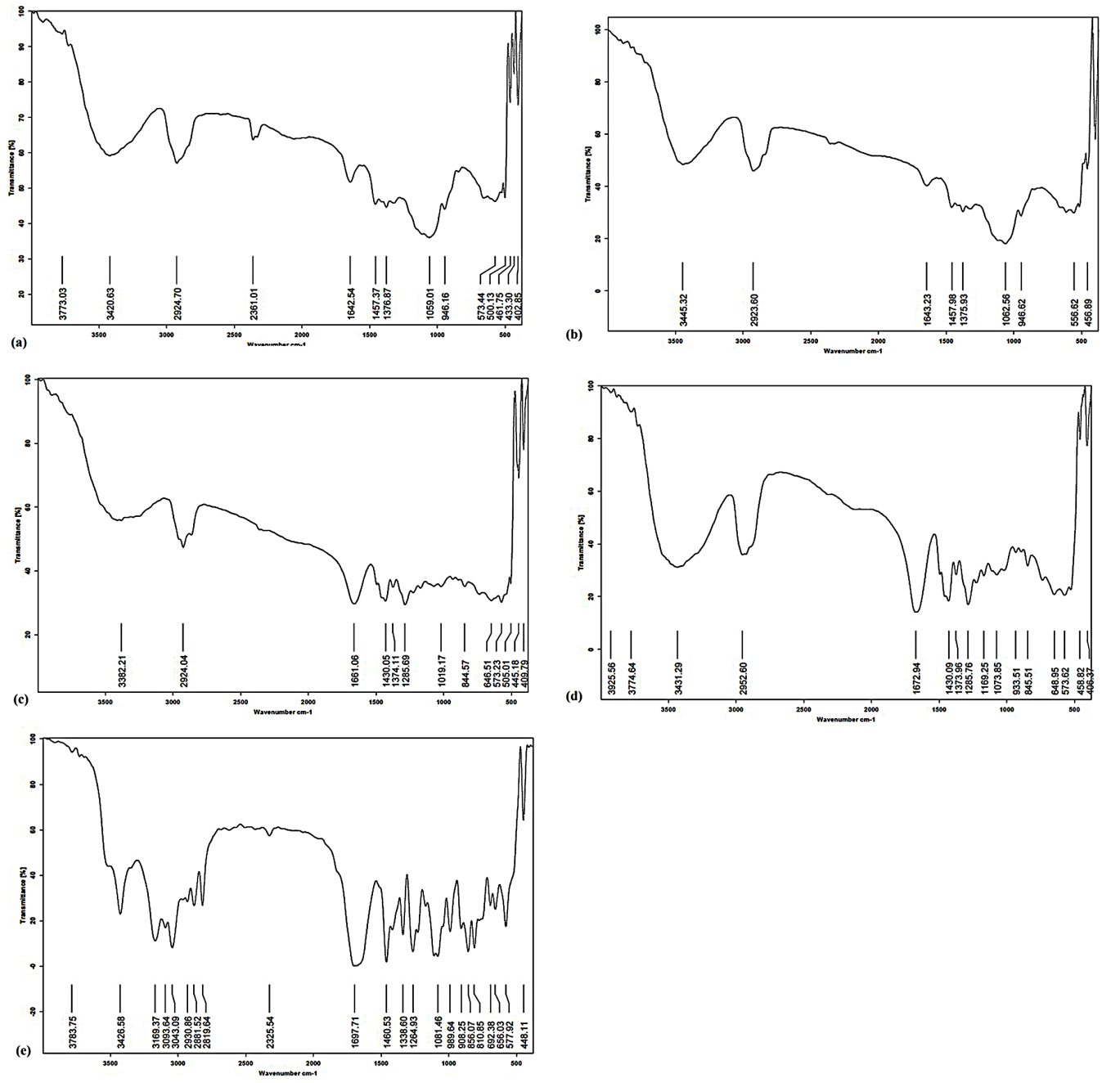

FIGURE 8 - FTIR spectra of (a) HPMC K15M, (b) HPMC K100, (c) PVP K30, (d) optimized formula, (e) pure drug.

Differential scanning colorimetry (DSC) study

The interaction between drugs and polymers can be predicted by the behaviour of the material with respect to change in temperature. DSC is a thermoanalytical technique in which the difference in the amount of heat required indicated in terms of appearance and disappearance of a peak for endothermal and exothermal peak with respect to increase the temperature of a sample and reference as a function of temperature is recorded (Gill, Moghadam, Ranjbar, 2010). In our study, DSC Universal V4.5A TA Instruments with nitrogen gas purging (50 ml/mnt) set to carry out the experiment. Figure 9 (a) illustrated a sharp peak for stavudine at

169.66 ^{0}C, corresponding to the melting point. An additional peak at 185.71 ^{0}C was also observed, could be a result of impurity. Similarly, the characteristic broad peak at 83.09 ^{0}C and 87.07 ^{0}C observed for HPMC K15M and HPMC K100 respectively. Figure 9(d) displayed the endothermal peak for an optimized formula with a slight change in a peak at 160.53 ^{0}C, whereas an additional peak at 72.76 ^{0}C for HPMC was marked. The result indicated, might be slight interaction, moisture or impurity in the presence of solvent in the optimized formula.

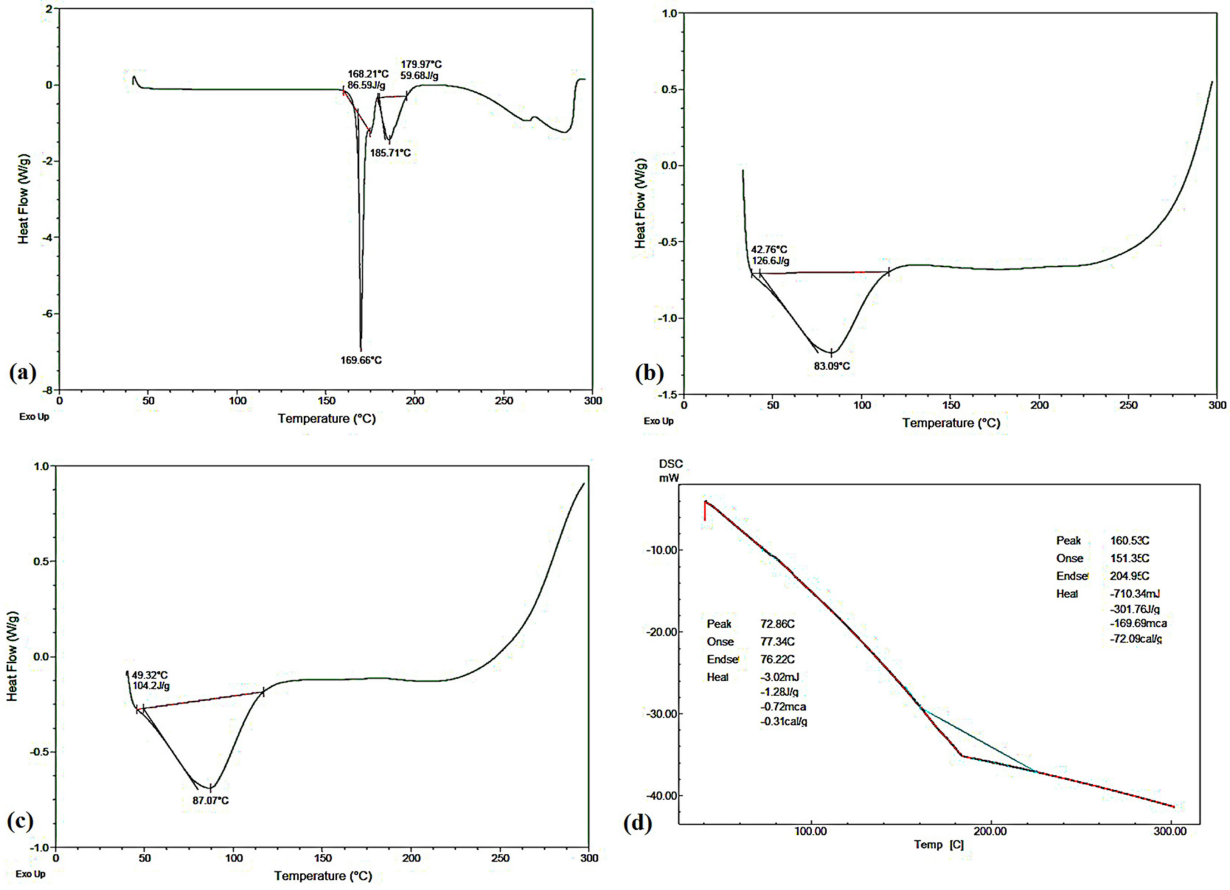

FIGURE 9 - DSC thermogram of (a) pure drug, (b) HPMC K15M, (c) HPMC K100, (d) optimized formulation.

X-ray diffraction study

In XRD, compound identification in relation to crystallographic change, preferred orientation used to characterize a crystalline substance (Lennox, 1957). In our study, the pure drug, HPMC K15M, HPMC K100, and optimized formula subjected to XRD 7000, Shimadzu. A voltage of 40.0 (kV) was applied during the entire scanning. The scanning mode was continuous with a speed of 4.00 (deg/min), and scan range 10.000-80.000 (deg). The pure drug provided a clear diffractogram with sharp and tall peaks. In XRD study, it received clear evidence of unique peaks at 10.96, 17.14, 17.22, 22.9, 24.66 and 28.37 ^{0}2θ for pure drug. HPMC K15M exhibited characteristic peak at 19.82 ^{0}2θ. Similarly HPMC K100 characterized by broad peak at 10.44 and 20.58 ^{0}2θ. The optimized formula mixture did not exhibit a remarkable change in crystallinity, but slightly broad and narrow peaks as well as intensity of peak decreased as seen in Figure 10, which could be the result of crystallinity change in the presence of solvent and storage condition.

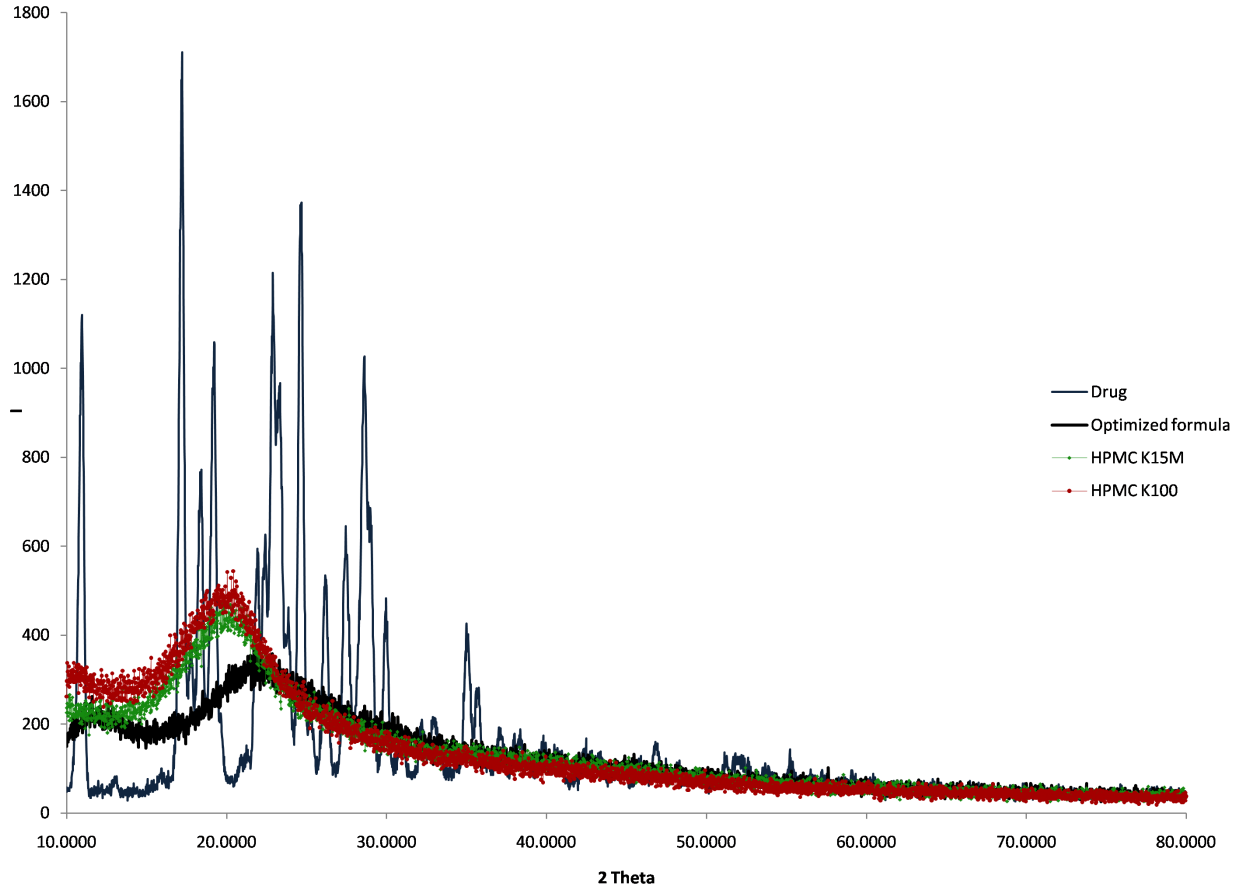

FIGURE 10 - Overlay XRD diffractogram for pure drug, optimized formula, HPMC K15M and HPMC K100.

CONCLUSION

Pharmaceutical industries involve a large amount of capital and human resource for developing drug and dosage forms. In the recent era, there has been a demand for the involvement of scientific treatment, especially *in-silico* methods. The manuscript focused on screening design followed by finding the best, termed as optimized formulation using in-silico technique and simulation by response surface method. During the study, a limited number of formulations anticipating the individual factors and their signifying effects on responses or dependent variables studied in mathematical and statistical approaches. In our study, it proved that from a limited number of twenty formulations, the responses from theoretical values were pretty much nearer to the predicted values. Moreover, the interaction study and characterization values from suggested CCD were acceptable. Furthermore, the *in-vivo* study can be carried out to find out the pharmacokinetic parameters.

ACKNOWLEDGMENT

Authors thanks to the management of Nirmala college of pharmacy and global institute of pharmaceutical education and research for providing research facilities to carry out the research project.

REFERENCES

Attia AK, Abdel-Moety MM, Abdel-Hamid SG. Thermal analysis study of antihypertensive drug doxazosin mesilate. Arab J Chem. 2017;10:S334-8.

Zerit (Stavudine). Available from: https://www.accessdata.fda.gov/drugsatfda_docs/label/2002/20412S017.pdf. [cited 2021 April 1].Arinkoola AO, Ogbe DO. Examination of experimental designs and response surface methods for

uncertainty analysis of production forecast: A Niger Delta case study. J Pet Eng. 2015;2015:16.

Aslani A, Sharifian T. Formulation, characterization and physicochemical evaluation of amoxicillin effervescent tablets. Adv Biomed Res. 2014;3:209.

Attia AK, Abdel-Moety MM, Abdel-Hamid SG. Thermal analysis study of antihypertensive drug doxazosin mesilate. Arab J Chem. 2017;10(Supplement 1):S334-8.

Aziz DE, Abdelbary AA, Elassasy AI. Implementing central composite design for developing transdermal diacerein-loaded niosomes: ex vivo permeation and in vivo deposition. Curr Drug Deliv. 2018;15(9):1330-42.

Baker TB, Smith SS, Bolt DM, Loh WY, Mermelstein R, Fiore MC, et al. Implementing clinical research using factorial designs: a primer. Behav Ther. 2017;48(4):567-80.

Baranov A, Muzyko E. Valuation of compound real options for investments in innovative projects in pharmaceutical industry. Procedia Econ. 2015;27:116-25.

Cheng L, Li T, Dong L, Wang X, Huo Q, Wang H, et al. Design and evaluation of bilayer pump tablet of flurbiprofen solid dispersion for zero-order controlled delivery. J Pharm Sci. 2018;107(5):1434-42.

Dokoumetzidis A, Kalantzi L, Fotaki N. Predictive models for oral drug absorption: from in silico methods to integrated dynamical models. Expert Opin Drug Metab Toxicol. 2007;3(4):491-505.

Durakovic B. Design of experiments application, concepts, examples: State of the art. Period Eng Nat Sci. 2017;5(3):421-39.

El-Helaly SN, Habib BA, El-Rahman M K. Resolution V fractional factorial design for screening of factors affecting weakly basic drugs liposomal systems. Eur J Pharm Sci. 2018;119:249-58.

Giaccotto C, Golec J, Vernon J. New estimates of the cost of capital for pharmaceutical firms. J Corp Finan. 2011;17(3):526-40.

Gill P, Moghadam TT, Ranjbar B. Differential scanning calorimetry techniques: applications in biology and nanoscience. J Biomol Tech. 2010;21(4):167-93.

Hardikar S, Bhosale A. Formulation and evaluation of gastro retentive tablets of clarithromycin prepared by using novel polymer blend. Bull Fac Pharm Cairo Univ. 2018;56(2):147-57.

Hasniyati MR, Zuhailawati H, Ramakrishnan S. A statistical prediction of multiple responses using overlaid contour plot on hydroxyapatite coated magnesium via cold spray deposition. Procedia Chem. 2016;19:181-8.

Hejaz H A, Karaman R. Drug overview. Commonly used drug. In: Rafik Karaman Ed. New York: Nova Science Publishers. 2015.; pp. 1-40.

Hooda A, Nanda A, Jain M, Kumar V, Rathee P. Optimization and evaluation of gastroretentive ranitidine HCl microspheres by using design expert software. Int J Biol Macromol. 2012;51(5):691-700.

Huang J, Wigent RJ, Schwartz JB. Drug–polymer interaction and its significance on the physical stability of nifedipine amorphous dispersion in microparticles of an ammonio methacrylate copolymer and ethylcellulose binary blend. J Pharm Sci. 2008;97(1):251-62.

Jaynes J, Ding X, Xu H, Wong WK, Ho CM. Application of fractional factorial designs to study drug combinations. Sta t Med. 2013;32(2):307-18.

Sah AK, Suresh PK. Loteprednol etabonate nanoparticles: optimization via Box-Behnken design response surface methodology and physicochemical characterization. Curr Drug Deliv. 2017;14(5):676-89.

Kassem M, El Shaboury K, Mohamed A. Application of central composite design for the development and evaluation of chitosan-based colon targeted microspheres and in vitro characterization. Indian J Pharm Sci. 2019;81(2):354-64.

Kazmi SR, Jun R, Yu MS, Jung C, Na D. In silico approaches and tools for the prediction of drug metabolism and fate: A review. Comput Biol Med. 2019;106:54-64.

Koradia K, Parikh R, Koradia D. Application of plackett and burman design for screenin g of factors affecting albendazole nanocrystals. Curr Nanomed. 2017;7(2):158-67.

Kyavars V, Subramanian S. Formulation development and characterization of dasatinib nanocrystals and optimization using response surface methodology. Int J Pharma Res Health Sci. 2018;6(1):2295-02.

Lee M, Choi M. The determinants of research and development investment in the pharmaceutical industry: focus on financial structures. Osong Public Health Res Perspect. 2015;6(5):302-9.

Lennox D. X-Ray Powder Diffraction Patterns of Some Organic Compounds. Anal Chem. 1957;29(10):1433-5.

Mishra N, Mishra M, Padh H. Formulation development and optimization of efavirenz loaded SLNs and NLCs using Plackett- Burman design and its statistical elucidation. Int J Pharma Res Health Sci. 2018;6(2):2379-88.

Onakpoya IJ, Heneghan CJ, Aronson JK. Delays in the post-marketing withdrawal of drugs to which deaths have been attributed: a systematic investigation and analysis. BMC Med. 2015;13:26.

This is an open-access article distributed under the terms of the Creative Commons Attribution License.

Onakpoya IJ, Heneghan CJ, Aronson JK. Post-marketing withdrawal of 462 medicinal products because of adverse drug reactions: a systematic review of the world literature. BMC Med. 2016;14:10.

Ooms F. Molecular modeling and computer aided drug design. Examples of their applications in medicinal chemistry. Curr Med Chem. 2000;7(2):141-58.

Osamura T, Takeuchi Y, Onodera R, Kitamura M, Takahashi Y, Tahara K, et al. Formulation design of granules prepared by wet granulation method using a multi-functional single-punch tablet press to avoid tableting failures. Asian J Pharm Sci. 2018;13(2):113-9.

Parhi R, Suresh P, Patnaik S. Application of response surface methodology for design and optimization of reservoir-type transdermal patch of simvastatin. Curr Drug Deliv. 2016;13(5):742-53.

Prasad PS, Imam SS, Aqil M, Sultana Y, Ali A. QbD-based carbopol transgel formulation: characterization, pharmacokinetic assessment and therapeutic efficacy in diabetes. Drug Deliv. 2016;23(3):1047-56.

Qu X, Venter G, Haftka R. New formulation of minimum-bias central composite experimental design and Gauss quadrature. Struct Multidiscipl Optim. 2004;28(4):231-42.

Rezende CA, Atta BW, Breitkreitz MC, Simister R, Gomez LD, McQueen-Mason SJ. Optimization of biomass pretreatments using fractional factorial experimental design. Biotechnol Biofuels. 2018;11:206.

Roy H, Nandi S. In-Silico Modeling in Drug Metabolism and Interaction: Current Strategies of Lead Discovery. Curr Pharm Des. 2019;25(31):3292-305.

Roy H. Box-Behnken Design for Optimization of Formulation Variables for Fast Dissolving Tablet of Urapidil. Asian J Pharm. 2018;12(3):S946-S954.

Sadhukhan B, Mondal NK, Chattoraj S. Optimisation using central composite design (CCD) and the desirability function for sorption of methylene blue from aqueous solution onto Lemna major. Karbala Int J Mod Sci. 2016;2(3):145-55.

Saini N, Bakshi S, Sharma S. In-silico approach for drug induced liver injury prediction: Recent advances. Toxicol Lett. 2018;295:288-95.

Sathish T, Kezia D, Bramhachari PV, Prakasham RS. Multi-objective based superimposed optimization method for enhancement of l-glutaminase production by Bacillus subtilis RSP-GLU. Karbala Int J Mod Sci. 2018;4(2018):50-60.

Shamsi M, Mohammadi A, Manshadi MK, Sanati-Nezhad A. Mathematical and computational modeling of nano-engineered drug delivery systems. J Control Release. 2019;307:150-65.

Simionato LD, Petrone L, Baldut M, Bonafede SL, Segall AI. Comparison between the dissolution profiles of nine meloxicam tablet brands commercially available in Buenos Aires, Argentina. Saudi Pharm J. 2018;26(4):578-84.

US National library of medicine. Pubchem: Stavudine. Available from: https://pubchem.ncbi.nlm.nih.gov/compound/Stavudine. [cited 2019 August 30].

Using METHOCEL cellulose ethers for controlled release of drugs in hydrophilic matrix systems. Available from: https://www.colorcon.com/cn/products-formulation/all-products/download/677/2554/34. [cited 2019 August 12].

World Health Organization. HIV AIDS: Key facts. Available from: https://www.who.int/news-room/fact-sheets/detail/hiv-aids. [cited 2019 September 18].

Yu XQ, Wilson AG. The role of pharmacokinetic and pharmacokinetic/pharmacodynamic modeling in drug discovery and development. Future Med Chem. 2010;2(6):923-8.

Zerit (Stavudine). Available from: https://www.accessdata.fda.gov/drugsatfda_docs/label/2002/20412S017.pdf. [cited 2021 April 1].

Received for publication on 19th December 2020
Accepted for publication on 29th August 2021